Received 9 November 2023; revised 7 December 2023; accepted 10 December 2023. Date of publication 13 December 2023; date of current version 30 January 2024.

Digital Object Identifier 10.1109/OJAP.2023.3342147

A Design of Dual-Polarized Composite Patch-Monopole Antenna With Reconfigurable Radiation Pattern

THANH TUNG PHUNG [1] (Member, IEEE), SON XUAT TA [1] (Senior Member, IEEE), KHAC KIEM NGUYEN [1] (Member, IEEE), AND NGHIA NGUYEN-TRONG [2] (Senior Member, IEEE)

[1] School of Electrical and Electronic Engineering, Hanoi University of Science and Technology, Hanoi 100000, Vietnam

[2] School of Electrical and Mechanical Engineering, The University of Adelaide, Adelaide, SA 5005, Australia

CORRESPONDING AUTHOR: S. X. TA (e-mail: xuat.tason@hust.edu.vn)

This work was supported by the Ministry of Science and Technology (MOST) of Vietnam under Grant NĐT/KR/23/11.

ABSTRACT This paper describes a design of dual-polarized composite patch-monopole antenna with reconfigurable radiation pattern. The design consists of a double differential-feed patch loaded with four vertical monopoles symmetrically. The monopoles are connected to or disconnected from the ground plane (GND) by changing the ON/OFF states of p-i-n diodes. By adjusting the connections between the monopoles and GND, the pattern reconfigurability (i.e., one widebeam and three narrow-beam modes) can be achieved for each polarization. The proposed antenna can switch the beam in two dimensions separately ($xz-$ and $yz-$ plane). The proposed antenna is characterized computationally and validated experimentally. The measurements result in an overlapping 10-dB return-loss bandwidth of $2.40 - 2.51$ GHz and a port-to-port isolation ≥ 20 dB in all the modes. In the far field, the prototype can deploy switched beam flexibility. Its radiation characteristics are confirmed by the far-field measurements, which shows the reconfigurable patterns for both polarizations.

INDEX TERMS Composite patch-monopole, reconfigurable pattern, dual-polarization, p-i-n diode switch.

I. INTRODUCTION

RECONFIGURABLE techniques have been one of the key drivers for innovation in antenna designs [1], [2]. Reconfigurable antennas can offer the flexibility in terms of operational frequency, radiation pattern and/or polarization. Due to the rapid development of the modern wireless communications, such as 5G, Internet of Things, wireless local area network, vehicle to everything, pattern-reconfigurable antennas have been receiving substantial attention. These antennas can direct the main beam to the desired coverage area, consequently, improving the signal-to-noise ratio and the capacity of wireless communication systems.

Due to advantageous features of low cost, compact size, and conformal ability, microstrip patch antenna [3] is one of preferred choices for the pattern-reconfigurable antennas. Furthermore, patch antennas can be easily incorporated with p-i-n diodes, varactors, radio-frequency microelectromechanical systems (RF-MEMS), ferrites, or liquid crystals for the structural alterations, and consequently, achieving the pattern flexibility. In recent years, there have been a large number of studies reporting the pattern-reconfigurable patch antennas, which might be divided into two groups: the first group includes the antennas with switchable broadside and conical patterns [4], [5], [6], [7], [8], [9], [10], [11], [12], [13]; the second group is the pattern-reconfigurable antennas with multi-directional beam [14], [15], [16], [17], [18], [19], [20].

Two main methods for establishing the switchable broadside and conical patterns are (i) two patches with different operational modes are co-located and incorporated with switching feed networks [6], [7], [9], [11]; (ii) two different modes of a patch are switched by controlling ON/OFF states of integrated p-i-n diodes [4], [5], [8], [10], [12], [13]. The patch antennas with two pattern modes, however, may be insufficient for use in some applications that demands the antenna with multi-directional beams.

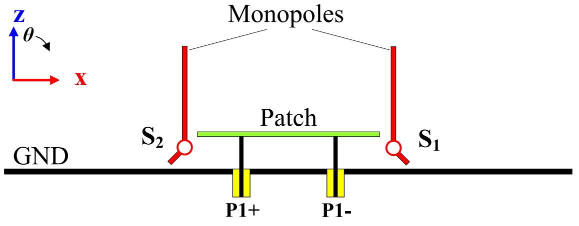

FIGURE 1. Schematic model of a differential feed patch antenna loaded with switchable monopoles.

The conventional patch antenna [3] yields a broadside radiation with narrow beamwidth (i.e., half-power beamwidths (HPBWs) of about 60° and 70° in the E- and H-planes, respectively). To realize the reconfigurable radiation pattern with multi-directional beam, the patch antenna has been loaded with alterable-shaped elements using p-i-n diodes, such as parasitic patches [14], [15], complementary split-ring resonator embedded on the ground plane [16], metasurfaces [17], and vertical metal walls [18], [19]. In [20], a square patch is incorporated with shorting pins and four varactors to generate continuous beam reconfigurability. These pattern-reconfigurable antennas with multi-directional beam, however, work for a single linear polarization. Under complex scenarios of the modern wireless communication systems, the single-polarized antenna may not effectively transmit/receive signals from mobile devices. To address this problem and enhance the capacity, antenna with dual-polarized radiation [21] has been considered as an effective solution. Accordingly, several patch antennas with dual-polarized and pattern-reconfigurable characteristics have been proposed. A two-port patch with ±45° dual-polarization [22] is loaded with two parasitic patches which are connected to/disconnected from the ground plane (GND) for pattern reconfigurability. In [23], a dual-port aperture-stacked patch antenna is incorporated with a pair of reconfigurable cross-shaped strips to bestow three-directional beams. These dual-polarized antennas yield the scanning beam in one dimension only.

In this paper, a design of dual-polarized composite patch-monopole antenna with reconfigurable radiation pattern is presented. In this design, we aim to achieve a large space coverage with higher gain for both polarizations. The antenna consists of a double differential-fed patch symmetrically loaded with four vertical monopoles which are connected to, or disconnected from the ground plane (GND) by changing the ON/OFF states of switches based on p-i-n diodes. By adjusting the p-i-n diode states, reconfigurable patterns can be achieved for both polarizations. For verification, an antenna operating at 2.45 GHz is designed, fabricated, and measured. Both simulation and measurement results illustrate that the proposed antenna achieves an improved coverage for both polarizations.

II. ANTENNA DESIGN AND CHARACTERISTICS

A. MECHANISM OF RECONFIGURABLE PATTERN

Fig. 1 shows the schematic model of a differential feed patch antenna symmetrically loaded with two vertical $\sim \lambda/4$ monopoles in the E-plane. The patch is designed to operate at TM_{10} mode. The monopoles can be connected to/disconnected from the GND by controlling ON/OFF states of two switches (S_1 and S_2). Accordingly, the antenna can operate in four modes (i.e., one widebeam and three narrow-beam modes), as given in Fig. 2.

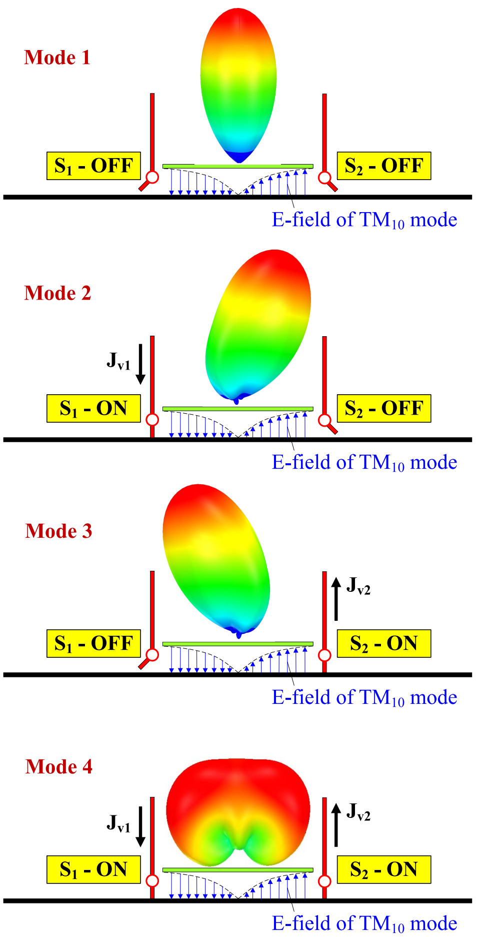

FIGURE 2. Mechanism of the pattern reconfigurability.

In Mode 1 with S1 and S2 OFF, the two monopoles are not induced by the patch, and consequently, the antenna operates as a conventional patch with the radiated field in E-plane [3] as follows:

$$E_{\text{patch}}(\theta) = E_1 \cos\left(\frac{\beta L}{2} \sin\theta\right) \tag{1}$$

where β is the propagation constant in free space, L is the patch length, and E_1 is the complex amplitude. Equation (1) indicates that the antenna working in Mode 1 yields a broadside unidirectional radiation.

In Modes 2 or 3 (S_1-ON and S_2-OFF/S_1-OFF and S_2-ON), one of the two monopoles is connected to the GND and inducted by the patch. The monopole with switch ON acts as a reflector, whereas the other one with switch OFF acts as a director. Accordingly, the main radiation beam of the antenna is tilted.

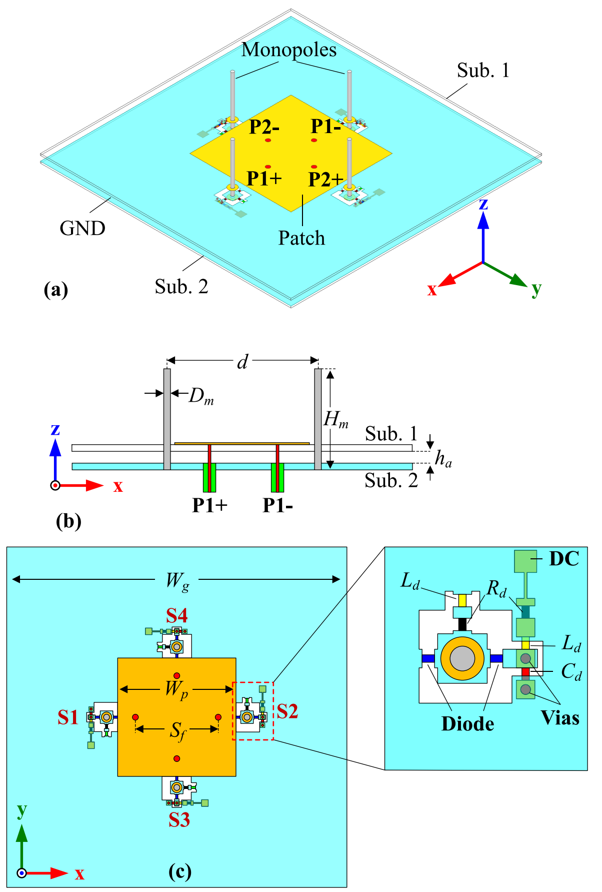

FIGURE 3. Geometry of propose antenna (a) Perspective view, (b) Cross sectional view, (c) Top view.

In Mode 4 with two switches ON, there are two vertical inducted currents (J_{v1} and J_{v2}) appear on the monopoles that have the same amplitude and opposite phase. In this state, the design works as the composite patch-monopole antenna whose total radiated field (E_{total}) can be synthesized as follows [24]:

$$E_{\text{total}}(\theta) = E_{\text{patch}} + E_{\text{monopole}} \times AF_{\text{monopole}} \tag{2}$$

where E_{monopole} is the radiation pattern of a monopole and AF_{monopole} is the array factor of these two monopoles. According to [3], the E-plane radiated field of a $\lambda/4$ monopole and AF_{monopole} of two monopoles with the same amplitude and opposite phase are given by:

$$E_{\text{monopole}}(\theta) = E_2 \frac{\cos(\frac{\pi}{2}\cos\theta)}{\sin\theta} \tag{3}$$

$$AF_{\text{monopole}}(\theta,\phi) = 2\sin\left(\frac{1}{2}\beta d \sin\theta\cos\phi\right) \tag{4}$$

where E_2 is the complex amplitude and d is the spacing between two monopoles. By adjusting the ratio of E_1/E_2, the composite patch-monopole antenna achieves a very wide beam in the E-plane ($\phi = 0°$) radiation pattern [24]. Since $AF_{\text{monopole}} = 0$ with $\phi = 90°$, the monopoles do not affect the H-plane pattern of the antenna.

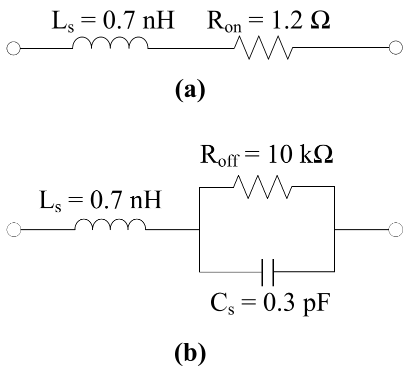

FIGURE 4. Equivalent circuit of p-i-n diode SMP1340-079: (a) ON-state, (b) OFF-state.

TABLE 1. Design parameters of the proposed antenna.

Par.	Value (mm)	Par.	Value (mm)	Par.	Value (mm)
S_f	22	d	56	W_p	48.5
H_m	24	h_a	2.4	D_m	1.5
W_g	120	h_{s1}	0.8128	h_{s2}	0.8128

B. GEOMETRY OF THE PROPOSED ANTENNA

Based on the conceptual design in Fig. 1, we propose a dual-polarized composite patch-monopole antenna with multiple-directional beam, as shown in Fig. 3. The antenna is composed of a double differential-feed square patch, four vertical monopoles, four switches ($S1 - S4$), two dielectric substrates (Sub. 1 and 2), and the GND. The patch is printed on the top side of Sub. 1, while the GND is placed on the top side of Sub. 2. The two substrates are Roger 4003 sheets ($\varepsilon_r = 3.38$, tan$\delta = 0.0027$, and thickness of 0.8128 mm), which are separated by an air-gap of h_a. The vertical monopoles are passed through Sub. 1 and connected to the GND via switches. A zoom-in view of a switch is illustrated in Fig. 3(c). Each switch consists of two p-i-n diodes, two resistors ($R_d = 100$ Ω), two inductors ($L_d = 56\ nH$), a capacitor ($C_d = 100\,pF$), and two shorting vias. The bias circuits are designed for ensuring forwarded-DC currents and RF-choke; i.e., the resistors are adopted to limit DC current follows to the diodes. The capacitor is to isolate the DC current, but allow flowing of the RF current (the impedance of capacitor is 0.64 Ω at 2.5 GHz). The inductors are used to isolate the RF currents (their impedances are 880 Ω at 2.5 GHz), but allow the forwarded DC current. Surface-mountable SMP1340-079 models from Skyworks Solutions [25] are selected for the pin diodes. In the full-wave simulations, the equivalent circuit of the diode is applied as in Fig. 4. To balance the inducted current on the monopoles, each switch needs two pin diodes. The proposed antenna is characterized using ANSYS Electronics Desktop for the center frequency of 2.45 GHz and its optimized design parameters are given in Table 1.

C. ANTENNA CHARACTERISTICS

As mentioned in Section II-A, the monopoles do not affect the $H-$plane pattern, and consequently, each pair of

TABLE 2. Radiation pattern of the antenna in eight modes.

Mode	Port excited	Switch ON	Switch OFF	Radiation patterns
1	P_{d1}	–	S_1, S_2	Broadside pattern with narrow beam
2	P_{d1}	S_1	S_2	Narrow-beam tilted to the $+x$ direction in xz plane
3	P_{d1}	S_2	S_1	Narrow-beam tilted to the $-x$ direction in xz plane
4	P_{d1}	S_1, S_2	–	Widebeam pattern in xz plane
5	P_{d2}	–	S_3, S_4	Broadside pattern with narrow beam
6	P_{d2}	S_3	S_4	Narrow-beam tilted to the $+y$ direction in yz plane
7	P_{d2}	S_4	S_3	Narrow-beam tilted to the $-y$ direction in yz plane
8	P_{d2}	S_3, S_4	–	Widebeam pattern in yz plane

switches (i.e., S_1-S_2 or S_3-S_4) can be used to control the radiation pattern in the *xz*- and *yz*-planes separately. The proposed antenna can operate in eight reconfigurable modes by switching ON and OFF states of the two pairs of switches. Its possible radiation patterns and the corresponding switch states are given in Table 2. It is noted that for Mode $1-4$, S_3 and S_4 do not affect the antenna performance and are set to be OFF (similarly for S_1 and S_2 for Mode $5-8$).

In the simulations, differential signals are applied to the two pairs of P_{1+}/P_{1-} and P_{2+}/P_{2-} (as shown in Fig. 3) for modeling the double differential feed (i.e., P_{d1} and P_{d2} ports). The differential S-parameters of the antenna can be calculated as follows [26]:

$$S_{d1d1} = \frac{1}{2}(S_{1+1+} - S_{1+1-} - S_{1-1+} + S_{1-1-}) \quad (5)$$

$$S_{d1d2} = \frac{1}{2}(S_{1+2+} - S_{1+2-} - S_{1-2+} + S_{1-2-}) \quad (6)$$

$$S_{d2d1} = \frac{1}{2}(S_{2+1+} - S_{2+1-} - S_{2-1+} + S_{2-1-}) \quad (7)$$

$$S_{d2d2} = \frac{1}{2}(S_{2+2+} - S_{2+2-} - S_{2-2+} + S_{2-2-}) \quad (8)$$

Fig. 5 shows the simulated $|S_{d1d1}|$ and $|S_{d2d2}|$ of the proposed antenna in different operating modes. In Modes 1 and 5, the antenna works as a conventional patch which yields a resonance at 2.46 GHz and 10-dB return loss bandwidth of $2.42 - 2.50$ GHz. When one or two monopoles are connected to the GND which generate extra-resonance for the antenna system, and consequently, broaden the impedance matching bandwidth [24]. In Modes 2, 3, 6, and 7, the antenna yields two resonances at 2.4 GHz and 2.58 GHz and an impedance matching bandwidth of $2.33 - 2.59$ GHz. With the two switches ON, it yields two resonances at 2.33 GHz and 2.60 GHz and a bandwidth of $2.27 - 2.64$ GHz for 10-dB return loss.

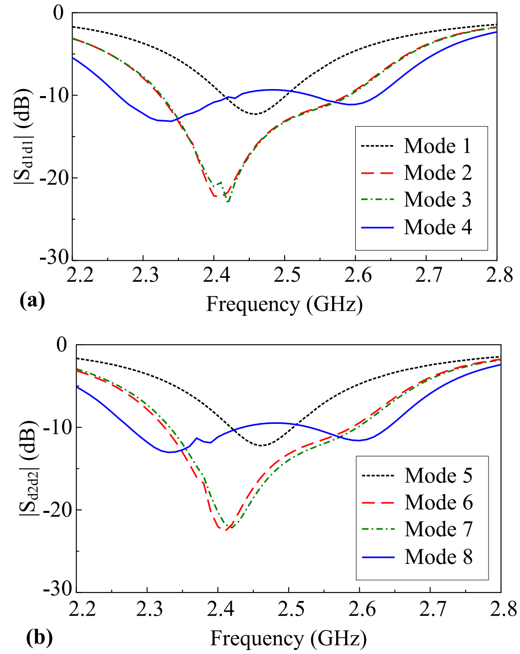

FIGURE 5. Simulated $|S_{d1d1}|$ and $|S_{d2d2}|$ of the proposed antenna in different operating modes.

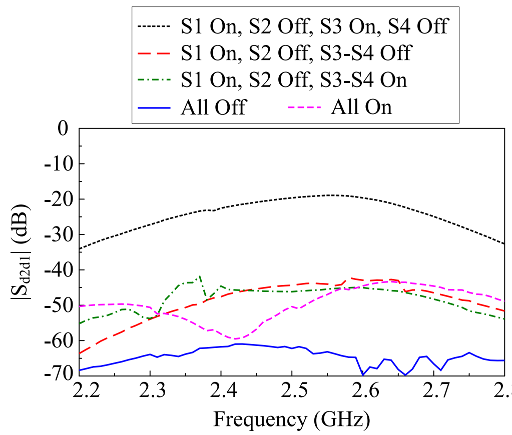

FIGURE 6. Simulated coupling coefficient of the proposed antenna.

The coupling coefficients among P_{d1} and P_{d2} ports are calculated using (6) and (7) and given in Fig. 6. As analyzed in [27], for double differential feed scheme, the antenna needs to exhibit a structural symmetry across two planes *xz* and *yz* for zero coupling. As shown in Fig. 6, the cases with structural symmetry achieve very small coupling coefficients of ≤ -43 dB which is due to the symmetry of switches. When one switch of the two pairs is ON (such as S_1 ON - S_2 OFF and S_3 ON - S_4 OFF), the antenna structure is asymmetrical and yields a less perfect coupling coefficient of ≤ -20 dB.

For better illustrating the reconfigurability, the contour 2D plot of the 2.45-GHz radiation patterns of the proposed antenna are simulated in the different operating modes and shown in Fig. 7. In these plots, the patterns are presented in 3rd definition of Ludwig [28], i.e., Co-polar (L3X)

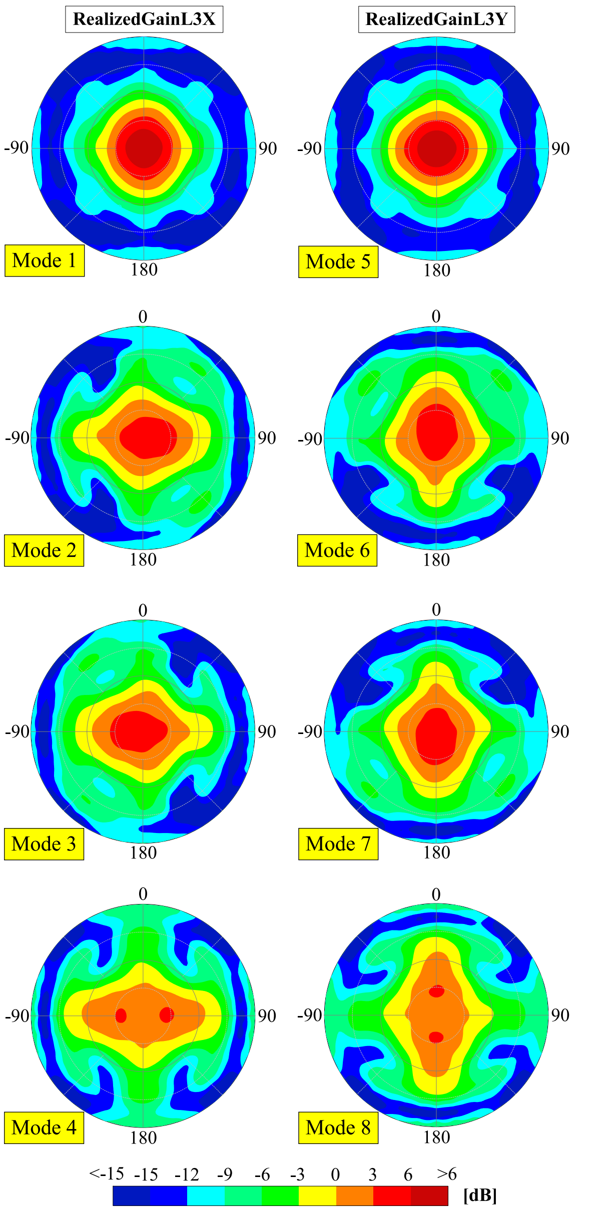

FIGURE 7. Contour 2D plots of 2.45-GHz radiation patterns of the proposed antenna in different operating modes. The range of θ is from 0° to 180° along the radius axis, while ϕ ranging from 0° to 360°.

for Mode 1−4 and Co-polar (L3Y) for Mode 5−8. It is observed that the antenna achieves multi-directional beam with extending coverage for both polarizations, i.e., x- and y-polarization. When the antenna is in Mode 1 (S_1 and S_2 OFF), the TM_{10} mode resonance is excited, and therefore, a broadside radiation with narrow beam is achieved for the $x-$polarization. For Mode 2, the left monopole is connected the GND via S_1 ON, the narrow-beam radiation pattern is deflected at $\theta = 25°$ in the xz-plane. For Mode 3, the right monopole is connected the GND via S_2 ON, the narrow-beam radiation pattern is deflected at $\theta = -25°$ in xz-plane. Based on the operation mechanism of a Yagi antenna, the deflecting angle is mainly determined by lengths (H_m) of reflector and director, and their spacing (d) over to the driven

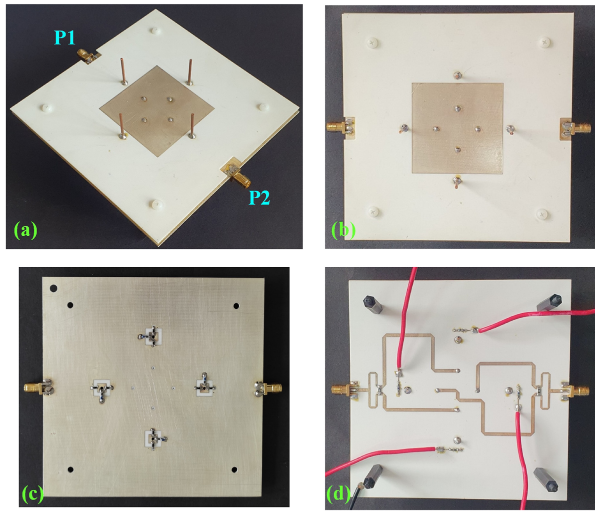

FIGURE 8. Fabricated prototype of the proposed antenna: (a) perspective view, (b) top view, (c) ground plane with switches, and (d) double differential feeding network and DC-bias.

element. In the proposed antenna, these parameters of H_m and d, however, considerably affect the impedance matching in the other modes (e.g., Modes 4 and 8). Accordingly, the $H_m = 24$ mm and $d = 56$ mm are chosen for the final design based on a tradeoff between the maximum deflecting angle and good impedance matching in all operation modes. When the antenna is in Mode 4, the two monopoles on the x axis are connected to the GND via S1 and S2 ON, which causes a widebeam radiation pattern in the xz plane. Similarly, the reconfigurability for the $y-$polarization is similar to the beam steerable along the yz-plane when the antenna is in Mode $5-8$, respectively. These results demonstrate that the proposed antenna achieves reconfigurable patterns with wide space coverage in both polarizations.

III. FABRICATION AND MEASUREMENTS

For verification, the dual-polarized composite patch-monopole antenna with reconfigurable radiation pattern is realized and measured. Fig. 8 shows a fabricated prototype of the antenna which has an overall size of 120 mm × 120 mm × 24 mm ($0.98\lambda_0 \times 0.98\lambda_0 \times 0.2\lambda_0$ at 2.45 GHz). The double differential feeding network consists of two Wilkison power divider and phase-delay lines, which is designed for the center frequency of 2.45 GHz. Plastic posts and screws are utilized to construct the antenna prototype. A 3-V battery is used to charge DC voltage to control the ON/OFF states of each switch. All DC wires are placed under the GND to avoid undesired effects on the antenna radiation.

Fig. 9 shows $|S_{11}|$ and $|S_{22}|$ values of the antenna prototypes in different operating modes. Both simulation and measurement indicate that the antenna yields a good impedance matching at the desired frequency band for all operating modes. Its whole pattern reconfigurable performances are yielded within the impedance matching bandwidth of 2.40 − 2.51 GHz for 10-dB return loss. Simulated and measured coupling coefficients of the prototype in different modes are illustrated in Fig. 10. In all cases

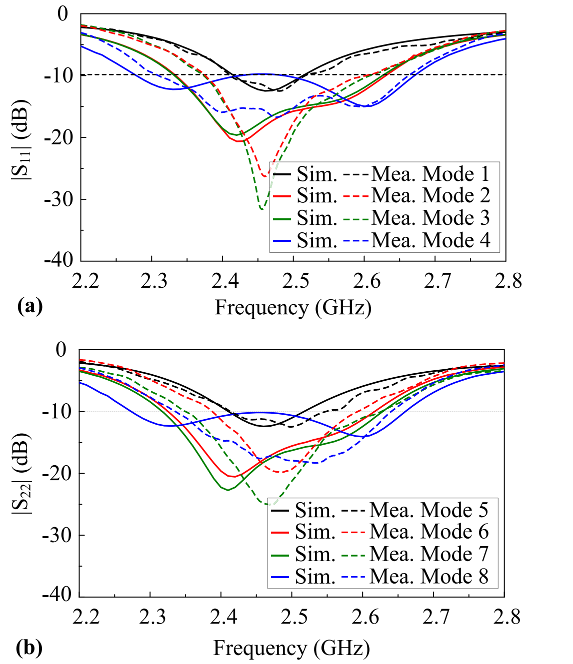

FIGURE 9. Simulated and measured reflection coefficients ($|S_{11}|$ and $|S_{22}|$) of the antenna prototype in different operating modes.

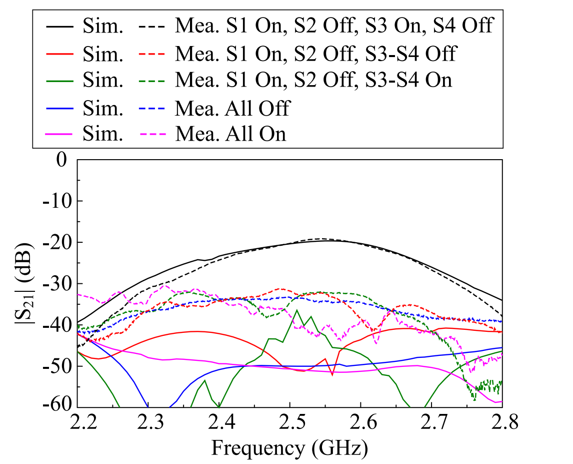

FIGURE 10. Simulated and measured coupling coefficients of the antenna prototype.

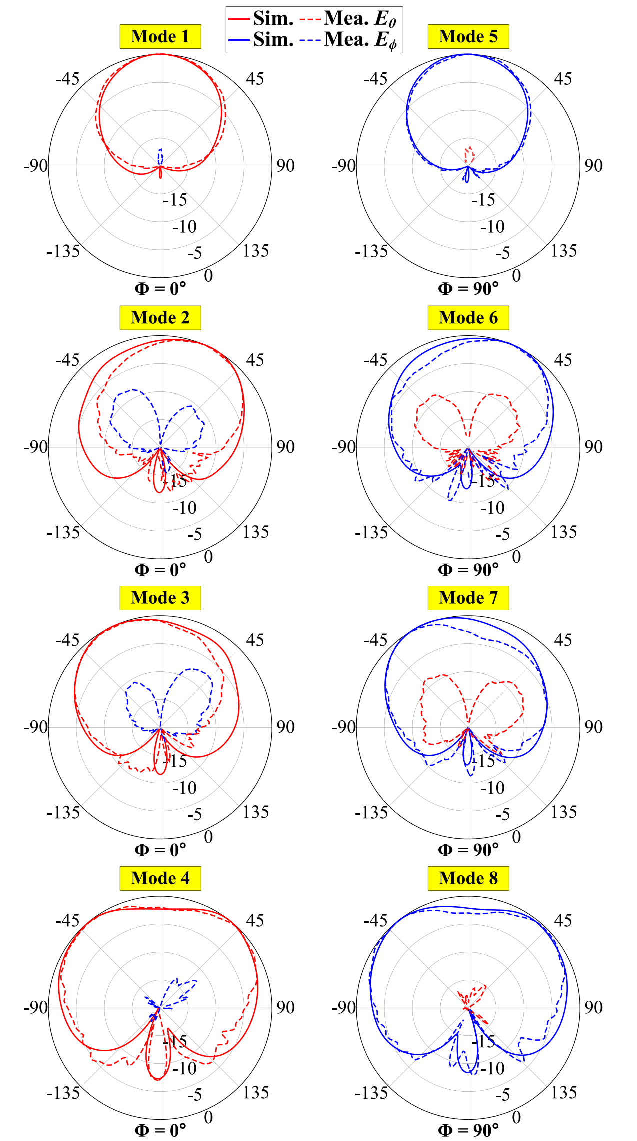

FIGURE 11. Normalized 2.45-GHz radiation pattern (in dB scale) of the antenna prototype in different modes.

with structural symmetry, the measured coupling coefficients are less than −30 dB. For the cases with asymmetric structure (such as S_1 ON - S_2 OFF and S_3 ON - S_4 OFF), within the operational bandwidth, both measured and simulated $|S_{21}|$ are still better than −20 dB. There is a slight discrepancy between the measured and simulated results in Figs. 9 and 10, which are attributed to small fabrication tolerances, imperfect feeding network, and tolerance of the pin diodes.

Fig. 11 shows the radiation patterns of the antenna prototype with different modes. There is a good agreement between the simulation and measurement which indicate that the antenna achieves the pattern reconfigurability for both polarizations. For each polarization, the antenna achieves multi-directional switchable beams, including three narrow-beam and one widebeam modes. When all switches are OFF (modes 1 and 5), the measurements result in broadside narrow-beam pattern with half-power beamwidth (HPBW) of 68° and cross-polarization level of ≤ -18 dB at the broadside direction. In Modes 2, 3, 6, 7, the narrow-beam radiation patterns are tilted to $\theta = \pm 25°$ in both xz and yz planes. These modes yield HPBWs of about 100° and cross-polarization level of about −10 dB. In these modes, the cross-polarization level is larger than other modes due to the asymmetric structure. When all switches are ON (mode 4 and 8), the antenna achieves a widebeam radiation pattern with HPBW of $\geq 160°$ and cross-polarization level of ≤ -19 dB at the broadside direction.

The peak realized gains of the fabricated prototype are given in Fig. 12. Again, the measurement results agreed rather closely with the simulations. Since the peak gain

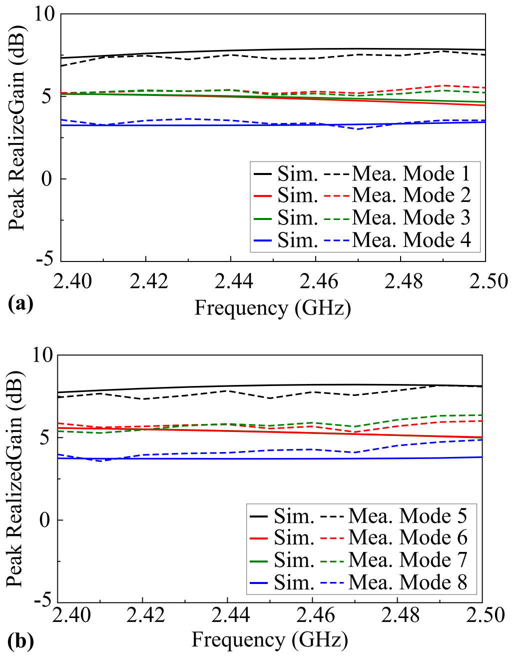

FIGURE 12. Peak realized gains of the antenna prototype in different modes: (a) P1 is excited, (b) P2 is excited.

TABLE 3. A comparison of the reconfigurable-pattern patch antennas with multi-directional beam.

Ant.	Overall size (λ_c)	Number of p-i-n diodes	Number of modes	Pol.	BW (%)
[14]	1.9 × 0.95 × 0.03	12	3	LP	3.22
[15]	0.95 × 0.95 × 0.013	4	9	LP	1.26
[16]	0.82 × 0.78 × 0.025	8	9	LP	2.45
[17]	1 × 1.12 × 0.12	6	12	LP	4.0
[18]	0.53 × 0.53 × 0.22	6	6	LP	10.8
[19]	0.83 × 0.83 × 0.21	8	3	LP	24.5
[22]	1.15 × 1.15 × 0.08	8	8	dual-LP	5.56
[23]	1.5 × 0.81 × 0.24	8	6	dual-LP	30.0
Prop.	0.98 × 0.98 × 0.2	8	8	dual-LP	4.5

BW: operational bandwidth; LP: linear polarization; λ_c is the free space wavelength referring to the center frequency.

and HPBW are inversely proportional, there is discrepancies in the peak gain between each operational mode. With the broadside narrow-beam pattern in Modes 1 and 5, the prototype achieves a measured peak gain of 7.0 dBi. For the tilted patterns in modes 2, 3, 6, and 7, the measurements result in the peak gains of about 5.3 dBi. In modes 4 and 8, the widebeam pattern is accompanied by a lower gain which is 3.4 - 3.9 dBi across the operational bandwidth. Due to the function limitation of the chamber, the radiation efficiencies of the antenna have not been measured. Nevertheless, since the measured gains are very close to the simulated values, the simulations should give a reasonable prediction of the efficiency of the prototype. In all operational modes of the proposed antenna, the simulations result in a radiation efficiency of greater than 90% across its operational bandwidth.

Table 3 shows a performance comparison between the proposed design and the reconfigurable-pattern patch antennas with multi-directional beam. Most of the priors, such as [14], [15], [16], [17], [18], [19], work for a single linear polarization. The dual-polarized antennas [22], [23] yield the scanning beam in one dimension. Different from [22], [23], our design targets to improve the gain coverage in the upper hemisphere for both polarizations, thus it provides scanning in two directions. As a result, the features of the proposed antenna include simple configurable, dual-polarization, reconfigurable pattern with multi-directional beam, and scanning beam in two dimensions.

IV. CONCLUSION

A dual-polarized composite patch-monopole antenna with reconfigurable radiation pattern has been described. It consists of a double differential-feed patch loaded with four vertical monopoles which are connected to the GND vias p-i-n based switches. By adjusting the ON/OFF states of switches, the multi-directional beam reconfigurability, including three narrow-beam and one widebeam modes, can be achieved for both x- and y-polarization. The final prototype with overall-size of $0.98\lambda_0 \times 0.98\lambda_0 \times 0.2\lambda_0$ at 2.45 GHz achieves a bandwidth of $2.40 - 2.51$ GHz in eight modes. For each polarization, the radiation pattern can be reconfigured to be either: (i) broadside narrow beam with HPBW of 68° and peak gain of 7.0 dB; (ii) titled narrow-beam at $\theta = 25°$ and peak gain of 5.3 dB; (ii) titled narrow-beam at $\theta = -25°$ peak gain of 5.3 dB; (iv) wide-beam with HPBW of $\geq 160°$ and peak gain of 3.7 dB. These features make the proposed antenna a promising candidate for modern wireless communication systems that require large coverage with polarization diversity.

REFERENCES

[1] C. G. Christodoulou, Y. Tawk, S. A. Lane, and S. R. Erwin, “Reconfigurable antennas for wireless and space applications,” *Proc. IEEE*, vol. 100, no. 7, pp. 2250–2261, Jul. 2012.

[2] J. Costantine, Y. Tawk, S. E. Barbin, and C. G. Christodoulou, “Reconfigurable antennas: Design and applications,” *Proc. IEEE*, vol. 103, no. 3, pp. 424–437, Mar. 2015.

[3] C. A. Balanis, *Antenna Theory: Analysis and Design*. Hoboken, NJ, USA: Wiley, 2015. [Online]. Available: https://books.google.com.vn/books?id=PTFcCwAAQBAJ

[4] P.-Y. Qin, Y. J. Guo, A. R. Weily, and C.-H. Liang, “A pattern reconfigurable u-slot antenna and its applications in MIMO systems,” *IEEE Trans. Antennas Propag.*, vol. 60, no. 2, pp. 516–528, Feb. 2012.

[5] S. Yan and G. A. E. Vandenbosch, “Radiation pattern-reconfigurable wearable antenna based on metamaterial structure,” *IEEE Antennas Wireless Propag. Lett.*, vol. 15, pp. 1715–1718, 2016.

[6] W. Lin, H. Wong, and R. W. Ziolkowski, “Wideband pattern-reconfigurable antenna with switchable broadside and conical beams,” *IEEE Antennas Wireless Propag. Lett.*, vol. 16, pp. 2638–2641, 2017.

[7] X. Ding, Z. Zhao, Y. Yang, Z. Nie, and Q. H. Liu, “A low-profile and stacked patch antenna for pattern-reconfigurable applications,” *IEEE Trans. Antennas Propag.*, vol. 67, no. 7, pp. 4830–4835, Jul. 2019.

[8] H.-W. Yu, Y.-C. Jiao, D.-Y. Li, and Z.-B. Weng, “A tm30-/tm40-mode pattern-reconfigurable microstrip patch antenna for wide beam coverage,” *IEEE Trans. Antennas Propag.*, vol. 67, no. 11, pp. 7121–7126, Nov. 2019.

[9] H. Sun, Y. Hu, R. Ren, L. Zhao, and F. Li, "Design of pattern-reconfigurable wearable antennas for body-centric communications," *IEEE Antennas Wireless Propag. Lett.*, vol. 19, pp. 1385–1389, 2020.
[10] K.-D. Hong, X. Zhang, L. Zhu, and T. Yuan, "A high-gain and pattern-reconfigurable patch antenna under operation of tm20 and tm21 modes," *IEEE Open J. Antennas Propag.*, vol. 2, pp. 646–653, 2021.
[11] C. X. Mao, L. Zhang, M. Khalily, and P. Xiao, "Single-pole double-throw filtering switch and its application in pattern reconfigurable antenna," *IEEE Trans. Antennas Propag.*, vol. 70, no. 2, pp. 1581–1586, Feb.2022.
[12] S.-T. Wang, L. Zhu, and H. Deng, "Design approach for pattern-reconfigurable patch antenna without extra feeding networks," *IEEE Trans. Antennas Propag.*, vol. 71, no. 2, pp. 1925–1930, Feb. 2023.
[13] G.-P. Gao, B.-K. Zhang, J.-H. Dong, Z.-H. Dou, Z.-Q. Yu, and B. Hu, "A compact dual-mode pattern-reconfigurable wearable antenna for the 2.4-GHZ WBAN application," *IEEE Trans. Antennas Propag.*, vol. 71, no. 2, pp. 1901–1906, Feb. 2023.
[14] X.-S. Yang, B.-Z. Wang, W. Wu, and S. Xiao, "Yagi patch antenna with dual-band and pattern reconfigurable characteristics," *IEEE Antennas Wireless Propag. Lett.*, vol. 6, pp. 168–171, 2007.
[15] M. Jusoh, T. Aboufoul, T. Sabapathy, A. Alomainy, and M. R. Kamarudin, "Pattern-reconfigurable microstrip patch antenna with multidirectional beam for wimax application," *IEEE Antennas Wireless Propag. Lett.*, vol. 13, pp. 860–863, 2014.
[16] Z.-L. Lu, X.-X. Yang, and G.-N. Tan, "A multidirectional pattern-reconfigurable patch antenna with CSRR on the ground," *IEEE Antennas Wireless Propag. Lett.*, vol. 16, pp. 416–419, 2017.
[17] M. A. Towfiq, I. Bahceci, S. Blanch, J. Romeu, L. Jofre, and B. A. Cetiner, "A reconfigurable antenna with beam steering and beamwidth variability for wireless communications," *IEEE Trans. Antennas Propag.*, vol. 66, no. 10, pp. 5052–5063, Oct. 2018.
[18] G. Yang, J. Li, D. Wei, S.-G. Zhou, and R. Xu, "Pattern reconfigurable microstrip antenna with multidirectional beam for wireless communication," *IEEE Trans. Antennas Propag.*, vol. 67, no. 3, pp. 1910–1915, Mar. 2019.
[19] J. A. Liu, Y. F. Cao, and X. Y. Zhang, "A pattern-reconfigurable filtering patch antenna using embedded resonators and switchable elements," *IEEE Trans. Antennas Propag.*, vol. 70, no. 5, pp. 3828–3833, May 2022.
[20] Z. Ding, R. Jin, J. Geng, W. Zhu, and X. Liang, "Varactor loaded pattern reconfigurable patch antenna with shorting pins," *IEEE Trans. Antennas Propag.*, vol. 67, no. 10, pp. 6267–6277, Oct. 2019.
[21] M. Mirmozafari, G. Zhang, C. Fulton, and R. J. Doviak, "Dual-polarization antennas with high isolation and polarization purity: A review and comparison of cross-coupling mechanisms," *IEEE Antennas Propag. Mag.*, vol. 61, no. 1, pp. 50–63, Feb. 2019.
[22] W.-Q. Deng, X.-S. Yang, C.-S. Shen, J. Zhao, and B.-Z. Wang, "A dual-polarized pattern reconfigurable yagi patch antenna for microbase stations," *IEEE Trans. Antennas Propag.*, vol. 65, no. 10, pp. 5095–5102, Oct. 2017.
[23] G. A. Ramírez et al., "Reconfigurable dual-polarized beam-steering broadband antenna using a crossed-strips geometry," *IEEE Antennas Wireless Propag. Lett.*, vol. 20, pp. 1379–1383, 2021.
[24] S. X. Ta, T. T. Phung, K. K. Nguyen, C. Dao-Ngoc, and N. Nguyen-Trong, "Low-profile dual-polarized composite patch-monopole antenna with broadband and widebeam characteristics," *IEEE Access*, vol. 11, pp. 87104–87110, 2023.
[25] "Data sheet of SMP1340-079 P-I-N diodes," Data Sheet SMP 1340, Skyworks Solut., Co., Irvine, CA, USA, 2019. [Online]. Available: https://www.skyworksinc.com/Products/Diodes/SMP1340-Series
[26] W. R. Eisenstadt, R. Stengel, and B. M. Thompson, *Microwave Differential Circuit Design Using Mixed-Mode S-Parameters*. Boston, MA, USA: Artech House, 2006.
[27] S. X. Ta and N. Nguyen-Trong, "Analysis and design of an ultrawideband dual-polarized antenna for IBFD applications," *IEEE Trans. Antennas Propag.*, vol. 70, no. 11, pp. 11121–11126, Nov. 2022.
[28] A. Ludwig, "The definition of cross polarization," *IEEE Trans. Antennas Propag.*, vol. 21, no. 1, pp. 116–119, Jan. 1973.

THANH TUNG PHUNG (Member, IEEE) is currently pursuing the B.Sc. (Eng.) degree in electronic and telecommunication engineering with the Hanoi University of Science and Technology, Vietnam, where he has been working as an Intership Researcher with the Communication Research and Development Laboratory since 2021. His research interests include microstrip patch antennas, dual-polarized antennas, multiband antennas, and reconfigurable antennas.

SON XUAT TA (Senior Member, IEEE) received the B.Sc. (Eng.) degree in electronics and telecommunications from the Hanoi University of Science and Technology, Vietnam, in August 2008, and the Ph.D. degree in electrical engineering from Ajou University, South Korea, in February 2016. From March 2016 to February 2017, he was a Postdoctoral Research Fellow with the Department of Electrical and Computer Engineering, Ajou University. From March 2017 to August 2017, he was with the Division of Computational Physics, Institute for Computational Science, and the Faculty of Electrical and Electronics Engineering, Ton Duc Thang University, Ho Chi Minh City, Vietnam. Since September 2017, he has been working as a Lecturer with the School of Electronics and Telecommunication (currently renamed as the School of Electrical and Electronic Engineering), Hanoi University of Science and Technology. He has authored and coauthored over 100 technical journal and conference papers. His research interests include antennas, metamaterials, metasurfaces, metamaterial-based antennas, metasurface-inspired antennas, circularly polarized antennas, and millimeter-wave antennas. He has served as a reviewer for over 20 scientific journals. He was selected as a Top Reviewer for IEEE TRANSACTIONS ON ANTENNAS AND PROPAGATION in 2020–2022.

KHAC KIEM NGUYEN (Member, IEEE) was born in Hanoi, Vietnam, in 1978. He received the B.Eng., M.Sc., and Ph.D. degrees from the School of Electronics and Telecommunication [currently renamed as the School of Electrical and Electronic Engineering (SEEE)], Hanoi University of Science and Technology (HUST), Vietnam, in 2001, 2003, and 2017, respectively. Since 2001, he has been working as a Lecturer with SEEE, HUST, and a Researcher with the CRD LAB, HUST. His research interests include design microstrip antenna for next-generation mobile communication systems as well as passive RF components.

NGHIA NGUYEN-TRONG (Senior Member, IEEE) received the Ph.D. degree (Doctoral Research Medal) in electrical engineering from The University of Adelaide, Adelaide, SA, Australia, in 2017.

He is currently a Lecturer with The University of Adelaide. His main research interests include microwave circuits, advanced materials, absorbers, and various types of antennas.

Dr. Nguyen-Trong was one of the recipients of the Best Student Paper Award at the 2014 IWAT, the 2015 IEEE MTT-S NEMO, and the 2017 ASA Conferences, and the Best Paper Award at the 2018 and 2020 AMS Conference. He has been continuously selected as a Top Reviewer for IEEE TRANSACTIONS ON ANTENNAS AND PROPAGATION in 2018–2021 and IEEE ANTENNA WIRELESS AND PROPAGATION LETTERS in 2018 and 2021. He serves as a Technical Co-Chair for the 2020 Australian Microwave Symposium (AMS) and 2022 IEEE International Symposium on Antennas and Propagation. He is listed among Australia's Top 40 Early Career Researchers by The Australian, November 2021.